Research Article J. Electrochem. Sci. Technol., 2017, 8(2), 101-106

Journal of Electrochemical Science and Technology
jecst.org

Surface Modification of a $Li[Ni_{0.8}Co_{0.15}Al_{0.05}]O_2$ Cathode using Li_2SiO_3 Solid Electrolyte

Jin Seo Park and Yong Joon Park*

Department of Advanced Materials Engineering, Kyonggi University, San 94-6, Iui-dong, Yeongtong-gu, Suwon-si, Gyeonggi, 443-760, Korea

ABSTRACT

Li_2SiO_3 was used as a coating material to improve the electrochemical performance of $Li[Ni_{0.8}Co_{0.15}Al_{0.05}]O_2$. Li_2SiO_3 is not only a stable oxide but also an ionic conductor and can, therefore, facilitate the movement of lithium ions at the cathode/electrolyte interface. The surface of the Li_2SiO_3-coated $Li[Ni_{0.8}Co_{0.15}Al_{0.05}]O_2$ was covered with island-type Li_2SiO_3 particles, and the coating process did not affect the structural integrity of the $Li[Ni_{0.8}Co_{0.15}Al_{0.05}]O_2$ powder. The Li_2SiO_3 coating improved the discharge capacity and rate capability; moreover, the Li_2SiO_3-coated electrodes showed reduced impedance values. The surface of the lithium-ion battery cathode is typically attacked by the HF-containing electrolyte, which forms an undesired surface layer that hinders the movement of lithium ions and electrons. However, the Li_2SiO_3 coating layer can prevent the undesired side reactions between the cathode surface and the electrolyte, thus enhancing the rate capability and discharge capacity. The thermal stability of $Li[Ni_{0.8}Co_{0.15}Al_{0.05}]O_2$ was also improved by the Li_2SiO_3 coating.

Keywords : Surface coating, Cathode, Lithium battery, Solid electrolyte

Received : 18 October 2016, Accepted : 14 February 2017

1. Introduction

Lithium-ion batteries are currently considered as the most efficient power source for a wide range of applications, such as small power-supply systems for portable electronic devices and large batteries for renewable energy-storage systems and electric vehicles [1-8]. Their electrochemical characteristics, such as capacity, rate capability, cycle life, and safety, are highly dependent on the cathode material [9-16]. Thus, the study of advanced cathodes has become one of the most important subjects in the development of high-performance lithium-ion batteries [17-21]. Ni-based cathode materials (e.g., $Li[Ni_{0.8}Co_{0.15}Al_{0.05}]O_2$) have received great attention because of their high discharge capacity and low cost. However, there are still problems such as low rate capability, unstable cyclic performance, and low thermal stability that must be overcome to achieve stable and high-performance lithium-ion batteries [22-25].

Surface modification by coating with stable materials (such as oxides, phosphates, and fluorides) is an effective approach to enhance the electrochemical performance of cathode materials [26-35]. AlF_3 [36], SiO_2 [37], and $Ni_3(PO_4)_2$ [38] have been used to modify the surface of Ni-based cathode materials. A stable coating layer can prevent undesired side reactions between the cathode and the reactive electrolyte, and improve the electrochemical properties and stability of the cathode material. In this study, Li_2SiO_3, a solid electrolyte with high ionic conductivity, was used as a coating material for the Ni-based cathode $Li[Ni_{0.8}Co_{0.15}Al_{0.05}]O_2$. Li_2SiO_3 coatings have been successfully applied to other cathode materials [39-41]. This solid-electrolyte coating is expected to facilitate the movement of lithium ions in the cathode interface and protect the surface of the cathode from the reactive electrolyte. Therefore, surface modification with Li_2SiO_3 may result in the formation of a stable coating

*E-mail address: yjpark2006@kyonggi.ac.kr

DOI: https://doi.org/10.5229/JECST.2017.8.2.101

layer with protective properties and lead to the enhancement of the rate capability and stability of the $Li[Ni_{0.8}Co_{0.15}Al_{0.05}]O_2$ cathode.

2. Experimental Section

Commercial pristine $Li[Ni_{0.8}Co_{0.15}Al_{0.05}]O_2$ (ECO-PRO) was used as the cathode material. The Li_2SiO_3 coating layer was prepared from an ethanol coating solution obtained by diluting lithium ethoxide and tetraethyl orthosilicate in ethanol. The mixture was stirred for 24 h at room temperature to obtain a homogeneous solution and the as-prepared $Li[Ni_{0.8}Co_{0.15}Al_{0.05}]O_2$ was then added. The mixture was heated to evaporate all of the solvent, and the residue was dried at 80°C for 24 h and then heated at 800°C for 1 h to obtain an amorphous Li_2SiO_3 coating layer. The coating amount was adjusted to either 0.25 wt% or 0.5 wt% of the pristine cathode.

Pristine and coated samples were characterized by X-ray diffraction (XRD, Rigaku) using monochromatic Cu Kα radiation (λ = 1.5406 Å), and their morphologies were observed by field emission scanning electron microscopy (FE-SEM, Nova Nano 200). For electrochemical testing, a cathode slurry was prepared by mixing $Li[Ni_{0.8}Co_{0.15}Al_{0.05}]O_2$ (pristine and Li_2SiO_3-coated), carbon black (Super P), and polyvinylidene fluoride in a weight ratio of 8:1:1, respectively. The mixed slurry was coated on the surface of an Al foil using a doctor blade and then dried at 90°C for 24 h. Coin-type cells (2032) were fabricated using a cathode, a separator, a Li-metal anode, and an electrolyte (1 M $LiPF_6$ in ethylene carbonate/dimethyl carbonate (1:1 v/v)). The cells were subjected to galvanostatic cycling (WonATech voltammetry system) over a 3.0-4.5 V voltage range at various charge-discharge rates. Impedance measurements were performed by applying an AC voltage (5 mV amplitude, 100 kHz to 0.1 Hz frequency range) using an electrochemical workstation (AMETEK, VersaSTAT 3). The thermal stability of the charged (4.5 V) electrodes was analyzed by differential scanning calorimetry (DSC, Mettler Toledo) using a high-pressure DSC pan.

3. Results and Discussion

Fig. 1 shows XRD patterns of the pristine and Li_2SiO_3-coated $Li[Ni_{0.8}Co_{0.15}Al_{0.05}]O_2$ powders. The pristine, 0.25 wt% coated, and 0.5 wt% coated samples showed the same diffraction patterns, and the peaks were well indexed to the typical -$NaFeO_2$ structure (space group: R-3m). The peaks attributed to Li_2SiO_3 were not detected in the XRD patterns of the coated samples, probably because of the low coating-material content. Clearly, the coating process did not affect the structural integrity of the $Li[Ni_{0.8}Co_{0.15}Al_{0.05}]O_2$ cathode.

To compare the surface morphologies before and after Li_2SiO_3 coating, the pristine and coated $Li[Ni_{0.8}Co_{0.15}Al_{0.05}]O_2$ powders were observed by SEM, as shown in Fig. 2. All three powders consisted of spherical-shaped particles that were composed of nano-sized granules (secondary particles). Whereas the pristine $Li[Ni_{0.8}Co_{0.15}Al_{0.05}]O_2$ sample showed smooth facets, the surface of the Li_2SiO_3-coated powders was covered with heterogeneous island-type particles (the coating layer is marked with red circles in Fig. 2), indicating that the Li_2SiO_3 was not distributed on the $Li[Ni_{0.8}Co_{0.15}Al_{0.05}]O_2$ surface as a film-type coating layer. The 0.5 wt% coated powder was covered with a greater amount of coating material than the 0.25 wt% coated sample. The amount of coating material can affect the electrochemical performance of the electrodes; as Li_2SiO_3 is an electrically non-conductive material, a thick coating layer can hinder the movement of electrons at the cathode/electrolyte interface.

Electrochemical measurement of the pristine and Li_2SiO_3-coated $Li[Ni_{0.8}Co_{0.15}Al_{0.05}]O_2$ electrodes was

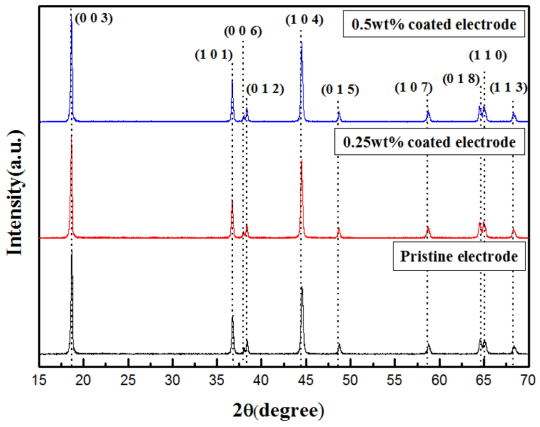

Fig. 1. XRD patterns of the pristine, 0.25 wt% Li_2SiO_3-coated, and 0.5 wt% Li_2SiO_3-coated $Li[Ni_{0.8}Co_{0.15}Al_{0.05}]O_2$ powders.

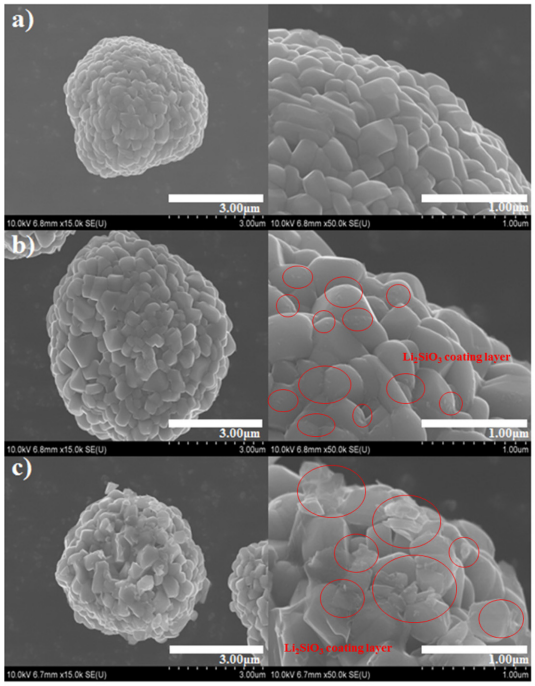

Fig. 2. SEM images of (a) pristine, (b) 0.25 wt% Li_2SiO_3-coated, and (c) 0.5 wt% Li_2SiO_3-coated $Li[Ni_{0.8}Co_{0.15}Al_{0.05}]O_2$ powders.

performed over a 3.0-4.5 V voltage range. Fig. 3a displays the discharge capacity and rate capability of the electrodes before and after surface modification. The cells were tested at current densities of 40, 100, 200, 600, and 1200 $mA \cdot g^{-1}$. After an initial fluctuation, the Li_2SiO_3-coated electrodes showed higher capacities than the pristine electrode at all current densities. The relatively higher capacities of the Li_2SiO_3-coated electrodes at high current densities suggest that the rate capability of the coated electrodes was superior compared to the pristine sample. Fig. 3(b-d) shows the discharge profiles at 40, 200, and 1200 $mA \cdot g^{-1}$, corresponding to the 5th, 25th, and 45th cycles shown in Figure 3a, respectively. At 40 $mA \cdot g^{-1}$, the capacities of the pristine, 0.25 wt% coated, and 0.5 wt% coated electrodes were ~191, ~208, and ~200 $mAh \cdot g^{-1}$, respectively. Thus, the difference in capacity among the samples was within 20 $mA \cdot g^{-1}$. At 1200 $mA \cdot g^{-1}$, the 0.25 wt% and 0.5 wt% Li_2SiO_3-coated electrodes showed reduced capacities of ~134 and ~123 $mAh \cdot g^{-1}$, respectively; yet these values were much higher than that of the pristine electrode, which dropped to ~99 $mAh \cdot g^{-1}$. Table 1 summarizes the discharge capacities and capacity retentions of the pristine and Li_2SiO_3-coated

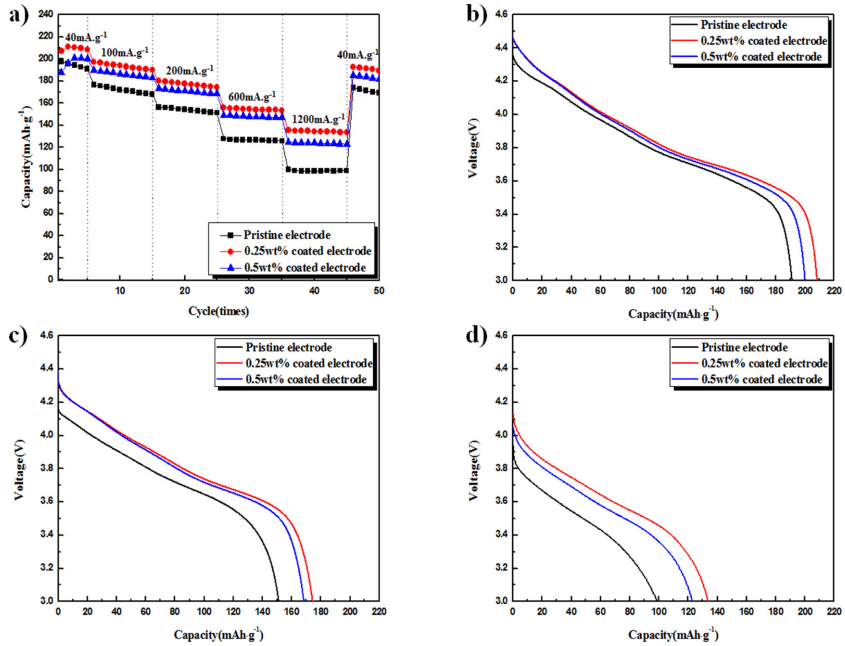

Fig. 3. (a) Discharge capacity of pristine and Li_2SiO_3-coated $Li[Ni_{0.8}Co_{0.15}Al_{0.05}]O_2$ at current densities of 40, 100, 200, 600, and 1200 $mA \cdot g^{-1}$, over a 3.0-4.5 V voltage range. Discharge profiles of the electrodes at (b) 40 $mA \cdot g^{-1}$, (c) 200 $mA \cdot g^{-1}$, and (d) 1200 $mA \cdot g^{-1}$.

Table 1. Discharge capacity and capacity retention of pristine and Li_2SiO_3-coated $Li[Ni_{0.8}Co_{0.15}Al_{0.05}]O_2$ at current densities of 40, 200, and 1200 $mA \cdot g^{-1}$. The percentages refer to the capacity retention at the 45th cycle compared with that at the 5th cycle.

Materials	40 $mA \cdot g^{-1}$	200 $mA \cdot g^{-1}$	1200 $mA \cdot g^{-1}$	Retention rate
Pristine electrode	191.2 $mAh \cdot g^{-1}$	151.2 $mAh \cdot g^{-1}$	99.0 $mAh \cdot g^{-1}$	50.2 %
0.25wt% coated sample	208.3 $mAh \cdot g^{-1}$	174.5 $mAh \cdot g^{-1}$	133.8 $mAh \cdot g^{-1}$	64.2 %
0.5wt% coated sample	200.1 $mAh \cdot g^{-1}$	168.5 $mAh \cdot g^{-1}$	123.0 $mAh \cdot g^{-1}$	61.5 %

samples. The capacity retention of the pristine electrode at 1200 $mA \cdot g^{-1}$ was ~50% of that measured at a current density of 40 $mA \cdot g^{-1}$, whereas the retention rates of the 0.25 wt% and 0.5 wt% coated electrodes were ~64 and ~61.5%, respectively. The enhanced discharge capacity and rate capability of the coated samples are attributed to the protective coating layer [28-35]. During cycling, the cathode surface is usually damaged by the electrolyte; small amounts of moisture in the electrolyte react with the fluoride salt to form HF, which attacks the cathode surface, resulting in the dissolution of transition metals and the formation of an undesired surface layer. The Li_2SiO_3 coating is electrically non-conductive, although it displays considerable ionic conductivity. Thus, a thick Li_2SiO_3 coating layer can hinder the movement of electrons during the charging/discharging process, which may decrease the capacity and rate capability of the coated electrodes. On the other hand, a thin layer or island-type nano-sized particles can reduce the direct contact between the cathode surface and the electrolyte, thus protecting the cathode surface against attack from the HF-containing electrolyte. The good ionic conductivity of Li_2SiO_3 may also facilitate the movement of lithium ions, thus contributing to the superior rate capability of the Li_2SiO_3-coated samples.

Impedance spectroscopy measurements confirmed the Li_2SiO_3 coating effect (Fig. 4). The Nyquist plots for all three electrodes show a semicircle in the mid- and high-frequency regions and a straight line in the low-frequency range. Each semicircle may be composed of two overlapped semicircles, one of which is related to the solid-electrolyte-interface impedance and the other to the charge-transfer resistance [29,42]. The diameter of the semicircle for the Li_2SiO_3-coated samples was smaller than that for the pristine electrode. Thus, we infer that the coating layer may influence the charge-transfer resistance as well as the impedance attributed to the solid-electro-

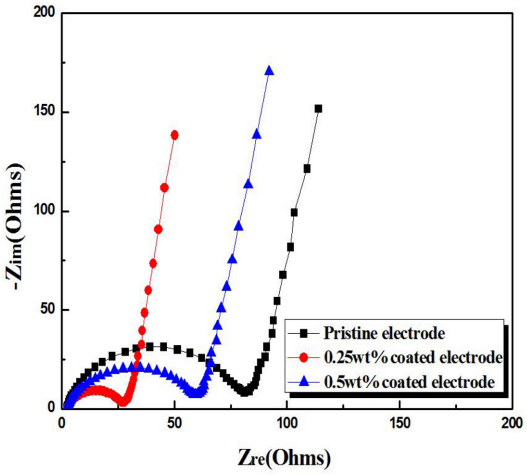

Fig. 4. Nyquist plots of the pristine and Li_2SiO_3-coated $Li[Ni_{0.8}Co_{0.15}Al_{0.05}]O_2$ electrodes.

lyte-interface. Because the semicircle diameter is an indication of the cell impedance, our results clearly show that the Li_2SiO_3 coating reduced the impedance of the electrodes. This is in agreement with the enhanced rate capability of the Li_2SiO_3-coated samples shown in Fig. 3. In particular, the superior rate capability of the 0.25 wt% coated electrode can be explained by its semicircle size, which is the smallest of the three electrodes.

Fig. 5 compares the cycling stability of the pristine and Li_2SiO_3-coated samples at a current density of 100 $mA \cdot g^{-1}$. The capacity of the coated samples was higher than that of the pristine electrode. However, in all cases, the capacity decreased during cycling and surface modification did not result in a clear improvement in the cyclic performance. The Li_2SiO_3 coating did, though, enhance the thermal stability of the charged electrode. Fig. 6 shows DSC profiles of the fully charged samples. The pristine electrode thermally reacted with the electrolyte at ~170°C, and the maximum exothermic peak was observed at ~237°C. The exothermic peaks of the Li_2SiO_3-coated

samples were clearly shifted to higher temperatures relative to the pristine electrode. In particular, the 0.5 wt% Li_2SiO_3-coated electrode showed the highest maximum exothermic peak temperature (~268°C), suggesting that a relatively thick coating layer is effective for improving the thermal stability. As shown in Fig. 3, the 0.25 wt% Li_2SiO_3 coating enhanced the rate capability of the electrode more than the 0.5 wt% coating, which indicates that a thick coating layer can hinder the movement of electrons. On the other hand, a sufficiently thick surface coating is required to enhance the thermal stability by reducing the contact area between the cathode and the electrolyte and, thus, prevent undesired exothermic reactions at the cathode/electrolyte interface.

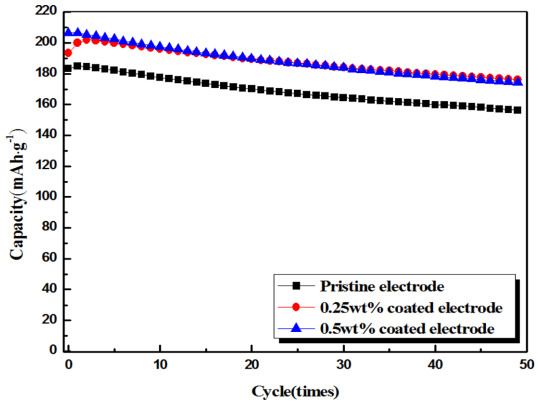

Fig. 5. Cyclic performances of the pristine and Li_2SiO_3-coated $Li[Ni_{0.8}Co_{0.15}Al_{0.05}]O_2$ electrodes.

4. Conclusion

In summary, the solid electrolyte Li_2SiO_3 was successfully used to coat a $Li[Ni_{0.8}Co_{0.15}Al_{0.05}]O_2$ cathode. The surface of the Li_2SiO_3-coated $Li[Ni_{0.8}Co_{0.15}Al_{0.05}]O_2$ cathode was covered with nano-sized Li_2SiO_3 particles, and the $Li[Ni_{0.8}Co_{0.15}Al_{0.05}]O_2$ structural integrity was not affected by the coating process. The Li_2SiO_3 coating increased the discharge capacity and rate capability of the $Li[Ni_{0.8}Co_{0.15}Al_{0.05}]O_2$ electrode,

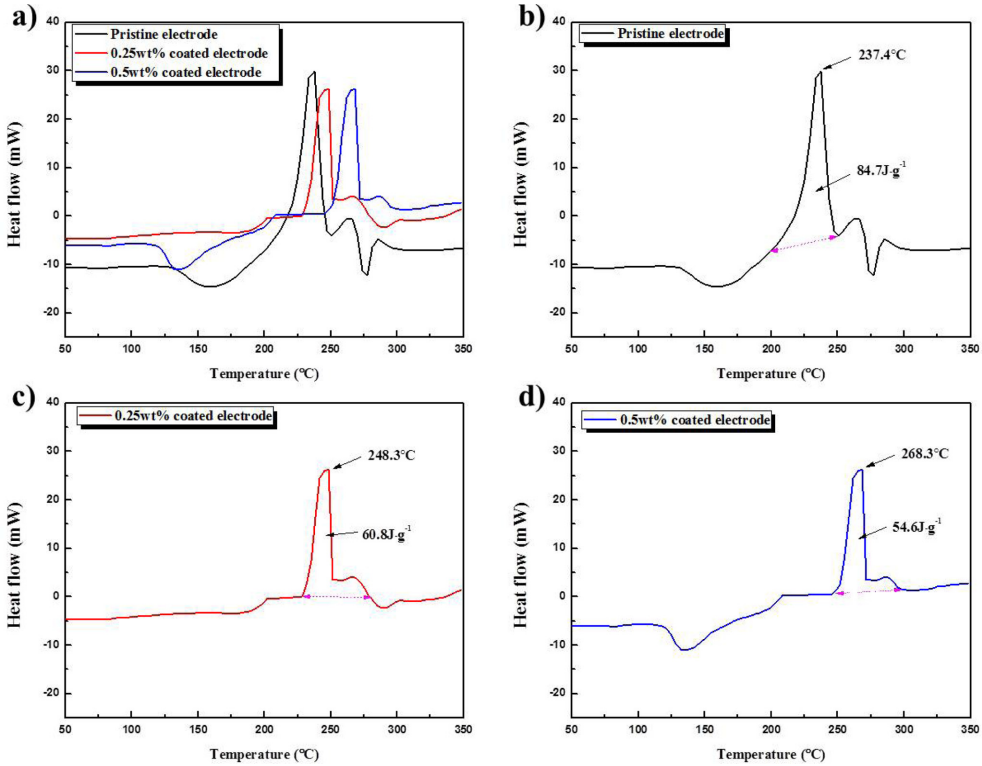

Fig. 6. (a) Superimposition of the DSC profiles of the (b) pristine, (c) 0.25 wt% Li_2SiO_3-coated, and (d) 0.5 wt% Li_2SiO_3-coated $Li[Ni_{0.8}Co_{0.15}Al_{0.05}]O_2$ electrodes.

indicating that the Li_2SiO_3 layer successfully prevents undesired side reactions between the cathode and the reactive electrolyte. Moreover, Nyquist plots showed that the Li_2SiO_3 coating decreased the impedance of the electrode, which suggests that the surface layer also stabilizes the $Li[Ni_{0.8}Co_{0.15}Al_{0.05}]O_2$ electrode/electrolyte interface. The Li_2SiO_3-coated samples also showed enhanced thermal stability compared to the pristine electrode. The 0.5 wt% Li_2SiO_3 coating was superior to the 0.25 wt% coating in terms of thermal stability, whereas the 0.25 wt% coated electrode showed superior rate capability.

Acknowledgments

This work was supported by Kyonggi University Research Grant 2015.

References

[1] S. Choi, J.B. Yoon, S. Muhammad and W.S. Yoon, *J. Electrochem. Sci. Technol.*, **2013,** *4(1),* 34-40.
[2] D. Jang, K. Palanisamy, Y. Kim and W.S. Yoon, *J. Electrochem. Sci. Technol.*, **2013**, *4(3)*, 102-107.
[3] C.K. Lee and Y.J. Park, *ACS Appl. Mater. Interfaces*, **2016**, *8(13)*, 8561-8567.
[4] J.M. Kim, M. Jeong, B.S. Jin and H.S. Kim, *J. Electrochem. Sci. Technol.*, **2014**, *5(1),* 32-36.
[5] S.W. Kim and K.Y. Cho, *J. Electrochem. Sci. Technol*., **2015**, *6(1),* 10-15.
[6] C.K. Lee and Y.J. Park, *Chem. Commun.*, **2015**, *51(7),* 1210-1213.
[7] D.H. Yoon, S.H. Yoon, K.S. Ryu and Y.J. Park, *Scientific Reports*, **2016**, *6*, 19962.
[8] D. Jang, K. Palanisamy, J. Yoon, Y. Kim and W.S. Yoon, *J. Power Sources,* **2013**, *244*, 581-585.
[9] J. Wang, W. Liu, S. Liu, J. Chen, H. Wang and S. Zhao, *Electrochim. Acta*, **2016**, *188*, 645-652.
[10] M.H. Pyun and Y.J. Park, *Nanoscale Research Letters*, **2016**, *11(1),* 272.
[11] X. Rui, O. Yan, M. Skyllas-Kzacos and T.M. Lim, *J. Power Sources*, **2014**, *258*, 19-38.
[12] M.H. Pyun and Y.J. Park, *J. Alloys Comp.*, **2015**, *643*, S90-S94.
[13] S. Watanabe, M. Kinoshita, T. Hosokawa and K. Morigaki, *J. Power Sources*, **2014**, *258*, 210-217.
[14] M.H. Pyun and Y.J. Park, *J. Electroceram*., **2014,** *33(3-4),* 264-271.
[15] Q. Li, G. Li, C. Fu, D. Luo, J. Fan and L. Li, *Appl. Mater. Interfaces*, **2014**, *6(13),* 10330-10341.
[16] L. Chen, Y. Su, S. Chen, N. Li, L. Bao, W. Li, Z. Wang, M. Wang and F. Wu, *Adv. Mater.*, **2014**, *26(39),* 6756-6760.
[17] C.S. Kim and Y.J. Park, *Solid State Ionics*, **2014**, *268*, 210-215.
[18] T. Wei, R. Zeng, Y. Sun, Y. Huang and K. Huang, *Chem. Commun.,* **2014**, *50(16),* 1962-1964.
[19] S.B. Lim and Y.J. Park, *Nanoscale Research Letters*, **2015**, *10(1),* 270.
[20] C.S. Kim, J.H. Cho and Y.J. Park, *Mater. Res. Bull.*, **2014**, *58*, 49-53.
[21] X. Xiang and W. Li, *Electrochim. Acta***, 2014**, *127*, 259-264.
[22] Y. Dai, L. Cai and R.E. White, *J. Power Sources*, **2014**, *247*, 365-376.
[23] Y. Chen, Y. Zhang, B. Chen, Z. Wang and C. Lu, *J. Power Sources*, **2014**, *256*, 20-27.
[24] K. Araki, N. Taguchi, H. Sakaebe, K. Tatsumi and Z. Ogumi, *J. Power Sources*, **2014**, *269*, 236-243.
[25] B. Huang, X. Li, Z. Wang, H. Guo, Z. He, R. Wang, J. Wang and X. Xiong, *Mater. Letters*, **2014**, *115*, 49-52.
[26] Y. Xu, Y. Liu, Z. Lu, H. Wang, D. Sun and G. Yang, *Applied Surface Sci.*, **2016**, *361*, 150-156.
[27] H.J. Lee and Y.J. Park, *Mater. Res. Bull*., **2014**, *58*, 169-173.
[28] H. Liu, C. Chen, C. Du, X. He, G. Yin, B. Song, P. Zuo, X. Cheng, Y. Ma and Y. Gao, *J. Mater. Chem. A*, **2015**, *3(6),* 2634-2641.
[29] H.G. Song, J.Y. Kim, K.T. Kim and Y.J. Park, *J. Power Sources,* **2011**, *196(16),* 6847-6855.
[30] X. Li, J. Liu, X. Meng, Y. Tang, M.N. Banis, J. Yang, Y. Hu, R. Li, M. Cai and X. Sun, *J. Power Sources*, **2014**, *247*, 57-69.
[31] H. J. Lee and Y.J. Park, *J. Power Sources***, 2013**, *244*, 222-233.
[32] B. Huang, X. Li, Z. Wang, H. Guo, X. Xiong and J. Wang, *J. Power Sources*, **2014**, *583*, 313-319.
[33] J. Shin, H. Jung, Y. Kim and J. Kim, *J. Alloys Compd*., **2014,** *589*, 322-329.
[34] H.J. Lee, K.S. Park and Y.J. Park, *J. Power Sources***, 2010**, *195(18),* 6122-6129.
[35] Y. Chen, K. Xie, C. Zheng, Z. Ma and Z. Chen, *Appl. Mater. Interfaces*, **2014**, *6(19),* 16888-16894.
[36] S.-H. Lee, C.S. Yoon, K. Amine and Y.-K. Sun, *J. Power Sources.,* **2013**, *234*, 201-207.
[37] Y. Cho and J. Cho, *J. Electrochem. Soc.*, **2010**, *157(6)*, A625-A629.
[38] D.J. Lee, B. Scrosati and Y.K. Suna, *J.Power Sources.,* **2011**, *196(18),* 7742-7746.
[39] E. Zhao, X. Liu, H. Zhao, X. Xiao and Z. Hu, *Chem. Commun*., **2015**, *51(44),* 9093-9096.
[40] K. Gao, S.X. Zhao, S.T. Guo, C.W. Nan, *Electrochim. Acta*., **2016**, *206*, 1-9.
[41] G. Hu, M. Zhang, L.Wu, Z. Peng, K. Du, and Y. Cao, *J. Alloys and Compounds*., **2017**, *690*, 589-597.
[42] G.T.-K. Fey, P. Muralidharan, C.-Z. Lu and Y.-D. Cho, *Solid State Ionics*, **2005**, *176(37),* 2759-2767.